ИНСТИТУТ ЯДЕРНОЙ ФИЗИКИ
им. Г.И. Будкера СО РАН

Yu.I. Belchenko, A.S. Kupriyanov

NEGATIVE HYDROGEN ION PRODUCTION IN THE HOLLOW CATHODE PENNING SPS

BUDKERINP 92-98

НОВОСИБИРСК

Negative Hydrogen Ion Production in the Hollow Cathode Penning SPS

Yu.I.Belchenko and A.S.Kupriyanov

Budker Institute of Nuclear Physics
630090, Novosibirsk, Russia

A B S T R A C T

A small hollow cathode Penning Surface-Plasma Source (SPS) was developed and studied. The H^- yield was proportional to the emission apertures area and was increased in a wide range of discharge current. The H^- yield with an intensity of up to 0.95 A and an emission current density of up to 3.6 A/cm^2 was obtained in pulsed mode. With the discharge current of 20 A and pulse duration of 60 sec an H^- yield with current of 0.1 A was obtained.

Dependencies of H^- yield vs magnetic field and a hydrogen feed were differed from that of the standard Penning SPS. An optimal cesium coverage of the electrodes was stable in the high-current long-pulsed operation as well as that in a dc source operation. The noticeable H^- production was realized with a low discharge voltage of 15 V. A low level of heavy negative ions less than 1% of total negative ion yield was obtained for the high-current long pulse operation. The yield of D^- ions had a 15% value lower than that of H^- ions at the high level of discharge current.

The most of extracted H^- ions were originated due to conversion of fast and superthermal (E > 1 eV) atoms on the cesiated surfaces of emission hole cones or due to the resonant charge-exchange of those anode-produced H^- ions in the vicinal volume of emission apertures.

1. INTRODUCTION

Ion sources with Penning geometry of electrodes are widely used for the production of Negative Ions (NI) since the well-known work of K.Ehlers [1]. An external magnetic field divides naturally the Penning discharge area into the "driver" and "extraction" regions with different electron temperatures. It provides an efficient volume production of NI in the pure-hydrogen Penning or Reflex-type NI sources, like that in the sources with special magnetic filter [2,3].

The Penning geometry of electrodes is also efficiently used in the surface-plasma sources of NI, where the most of NI are originated on the surfaces of electrodes being in contact with gas-discharge plasma. The high efficiency of NI production in the hydrogen-cesium Penning discharge and a very low energy spread of H^- ions extracted was found first by Belchenko and Dimov in November, 1971 during study of NI emission from planotron and Penning discharges [4,5]. This first Penning SPS (A in Fig. 1) was naturally introduced while an elimination of the central cathode plate from planotron (B in Fig. 1). The H^- yield from this first Penning SPS had an unexpectedly high value of up to 20 mA with the corresponding H^- current density of 0.4 A/cm^2. Further optimization of Penning SPS geometry increased the H^- emission current density up to the level of 1.5 A/cm^2, sufficient for an accelerator use [4,5].

Both fundamental facts: high H^- output and low energy spread of ions extracted were effectively used in further designs of Penning SPS model [6, 7] and in the first "industrial", reliable high-luminosity Penning SPS, developed by Dimov, Derevyankin and Dudnikov [8] and by Allison [9] for the long-term accelerator use.

The interest to Penning SPS H^- production mechanism increased during the study of hollow cathode Penning SPS with an independent NI emitter made by Belchenko and Dimov [10]. In this hollow cathode Penning SPS (C in Fig. 1) both cathodes were too distant from the emission slits region, so the cathode-produced NI and the corresponding contribution of volume charge-exchange of cathode-produced ions could not provide a significant H^- yield. But an H^- yield with an emission current density up to 2 - 2.7 A/cm^2 was recorded while studying this hollow cathode Penning SPS with an eliminated "independent emitter". It was suggested that an intense H^- yield in this source is caused by the surface-plasma production, but the detailed study of the anode emission mechanism had not been done.

Recently an interest to an anode surface-plasma NI production mechanism was additionally increased with the discovery of the enforced NI anode emission in the multicusp "volume" sources with adding barium or cesium [11,12].

A new small hollow-cathode Penning SPS with a multiaperture extraction has been fabricated in Novosibirsk for the anode NI production study. The source operates in either the pulse or dc mode. The influence of hydrogen pressure, of magnetic field, of emission plate temperature and potential bias on H^- production rate were studied. Experiments have been conducted to find out the dominant process involved into H^- production. It was found, that the anode surface conversion of superthermal and fast hydrogen atoms into H^- ions is effectively realized in the Penning SPS in the case of an increased, cesiated anode surface. The developed small version of hollow cathode Penning SPS produces the H^- beam with an intensity of up to 0.95 A and an emission current density of up to 3.6 A/cm^2. The cesium coverage of electrode surface and H^- emission rate were stable during the long-term source operation.

2. EXPERIMENTAL SETUP

A schematic of Hollow Cathode Penning (HCP) source is shown in Fig. 2. The principal geometry of electrodes was

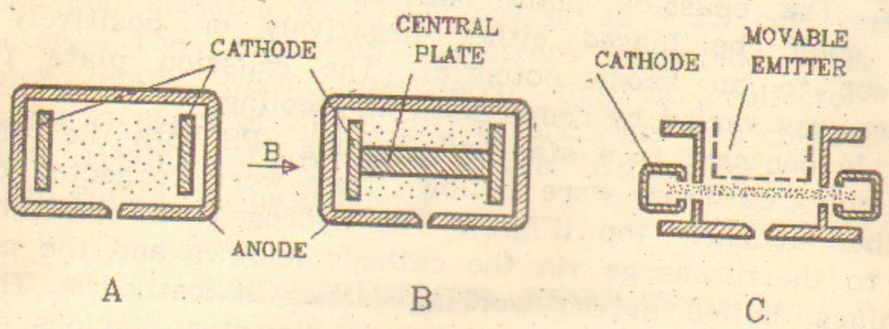

Fig.1. Penning (A), planotron (B) and hollow cathode Penning (C) surface plasma sources.

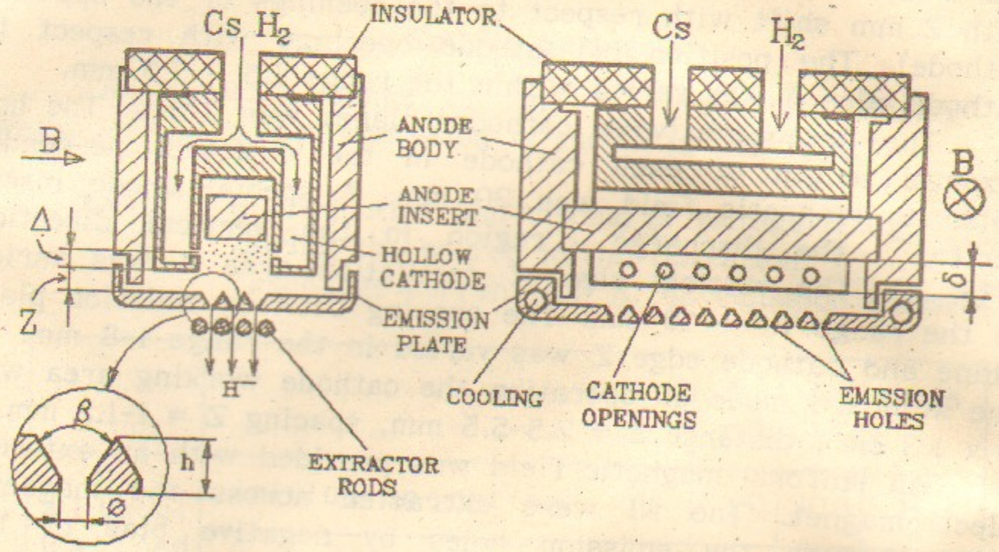

Fig.2. Cross sections of the hollow-cathode Penning source
left – along magnetic field;
right – across magnetic field.

similar to the standard Penning SPS, developed for accelerator use. The source chamber consists of a thick-walled rectangular anode body, ended by a 2-mm thick emission plate. The emission plate had an anode potential, but it also could be biased either negatively or positively with respect to an anode potential. The emission plate temperature was varied by compressed air cooling.

In contrast to a standard Penning SPS both the tantalum (or moly) cathodes were hollow. They were connected one to another at their top (Fig.2). The hydrogen and cesium were fed to the discharge via the cathode hollows and the cathode openings drilled in the working planes of cathodes. The cathode openings were 0.8 - 1 mm in diameter. Various number of cathode openings was used: 6 (3 at each cathode drilled with 8 mm step), 12 (6 at each cathode drilled with 4 mm step and located opposite to the openings of another cathode on the same magnetic field line) and 13 openings (6 at one and 7 at other cathode, drilled with 4 mm step and situated with 2 mm shift with respect to the openings of the opposite cathode). The position of cathode openings with respect to cathode edge Δ was varied within the range 1.5 - 7.5 mm.

The distance between cathodes planes was 8 mm. The horizontal length of each cathode in the direction perpendicular to magnetic field was 30 mm. A special anode insert limited the discharge region in the vertical direction (Fig. 2). The vertical size of oscillation area δ was varied in the range 1.5 - 10 mm. The spacing between emission plate plane and cathode edge Z was varied in the range 1-8 mm. In the standard mode of operation the cathode working area was 2×1.3 cm^2, distance Δ = 2.5-5.5 mm, spacing Z = 1-1.5 mm.

An uniform magnetic field was provided with an external electromagnet. The NI were extracted across the magnetic field through the emission holes by negative bias of the source body with respect to extractor. The extractor was made of tungsten rods, springed at their ends for thermal stability. Sizes, profile and the number of emission holes were varied during the source study. With the reversed, positive potential of the source body the positive ions were extracted from the source.

The mass composition of extracted positive and negative

ion beams was detected by small magnetic analyzer, moving across the beam. The total current in the extractor circuit was also monitored. The H^- beam was measured by movable Faraday cup situated at a distance of 15 - 25 cm from the extractor. The secondary electrons emitted from the collector plate were intercepted by the collector side walls. An accuracy of NI beams measurements was checked with a wide biasing of collector plate with respect to the grounded shield of the collector.

3. EXPERIMENTAL RESULTS

The best Hollow Cathode SPS NI production was achieved after plasma enhanced activation of the source surfaces. The maximum H^- yield was realized at maximum value of discharge current and at the optimal values of magnetic field, hydrogen pressure and emission plate temperature.

3.1. Source activation

The typical change of the H^- production during the source initial pulsed operation is shown in the Table 1.

Table 1. H production and discharge voltage change during the source initial operation. Discharge current 100 A. 48 emission holes.

		I^- mA	U_d V	Mode
without Cs feed	initial operation	10	300	H-I
	initial operation	40	300	H-II
with Cs	after Cs injection	100	150	HC-II
	after plasma activation	300	220	HC-I

A pure-hydrogen volume H^- production with H^- emission current density of 40 mA/cm^2 was obtained during the initial operation of the source with no Cs (discharge mode H-1). After electrode conditioning the discharge properties were changed. The growth of electrode temperature increased the surface H^- production in hydrogen discharge mode H-II [13] due to a diffusion of small amounts of cesium compounds to the electrode surfaces (line 2 of Table 1). An external injection of cesium (about 10^{-2} gram) led to an additional increase of H^- yield (line 3 in Table 1, mode HC-II). With further conditioning of the source in the hydrogen-cesium mode the H^- yield was substantially increased with a decrease in volume cesium density (discharge mode HC-1). The plasma enhanced activation of the source is clearly indicated to a surface production of the initial flux of H^- ions.

3.2. Multi-aperture H^- extraction

Some dependencies of extracted NI yield, obtained with the basic source geometry and pulse lengths 0.3 - 0.75 msec, as well as the dependence of discharge voltage U_d for mode HC-I are shown in Fig. 3. Curves I-III show the dependencies of NI yield on the discharge current for the hydrogen-cesium mode HC-I in the case of various number of emission holes or slits. Curve I was obtained with the NI extraction through 3 emission slits (1 × 17 mm^2 each, drilled with a 3 mm step). Curve II - extraction through 51 conical emission holes with 1.2 mm in diameter, drilled on the emission plate area 7.2 × 25.2 mm^2 in a three parallel rows. Curve III - extraction through 48 conical holes with 0.8 mm in diameter.

The majority of NI extracted (95-97%) were H^- ions. The H^- yield was invariable during the pulse length. The H^- yield was increased with the growth of discharge current up to 700 A (Mo cathode). In the case of tantalum cathodes (I.II in Fig. 3) the maximum value of the discharge current was limited by the cathode sparking.

The H^- yield was increased with the growth of permeable areas of emission holes. The maximal H^- yield with current

of up to 0.95 A was recorded while using 3 slits extraction at discharge current of 250 A. The H^- emission current density was maximal and had the abnormally high for Penning SPS value of up to 3.6 A/cm^2 in the case III for the Moly cathode (discharge current 700 A, pulse duration 0.3 msec). A corresponding average H^- current density in the formed beam after extractor had the value of up to 0.22 A/cm^2.

The most efficient H^- ion production was recorded for the low value of discharge current with a reduced voltage of hydrogen-cesium discharge mode HC-I (Fig. 3). The power efficiency $\lambda = I^-/ U_d I_d$ of H^- ion production (H^- yield normalized per discharge power) had the maximum value of λ = 0.12 A/kWt for discharge current 20 A and discharge voltage 60 V (3 slit extraction). This value of Penning SPS power efficiency was about 5 times lower, than that recorded for cathode H^- production in a grooved or honeycomb semiplanotron with an increased cathode surface and voltage [14]. The low value of discharge voltage of hollow cathode Penning SPS is important with respect to a lower rate of the cathode material sputtering.

3.3. Heavy ions

A low level of Heavy Negative Ions (HNI) (O^-, OH^-, etc) was recorded in the HCP extracted NI yield. A HNI current was increased in the first 0.3 msec of the pulse and decreased to the end of the pulse with a decrement of about 1 msec. The peak value of HNI fraction was about 3 - 5% of the total NI yield for the short-pulse operation. A HNI fraction was less than 1% of the total NI yield in the case of the long pulse operation.

The measurements of the composition of the positive ion current extracted with the reversed extraction voltage were made. At discharge current of 50 A about 60% of positive ion current were H^+ ions and the rest were H_2^+, H_3^+ and heavy positives. At discharge current 200 A a fraction of H^+ ions was increased up to 70%.

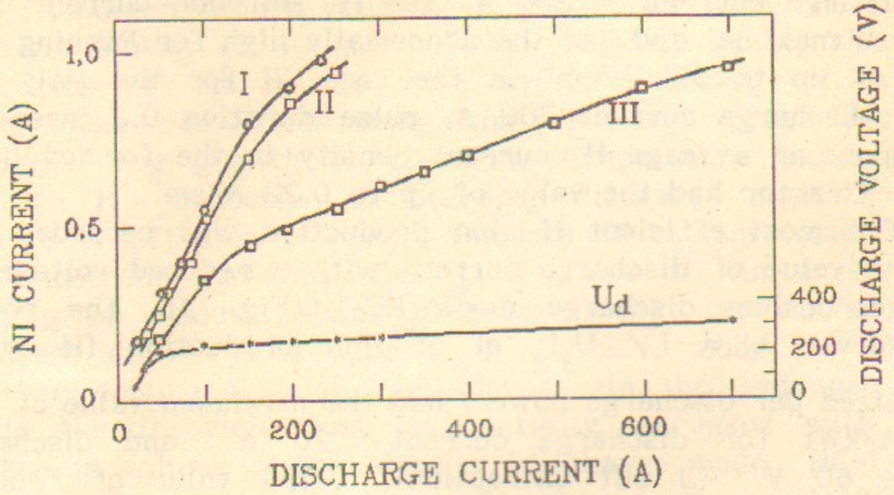

Fig.3. Dependencies of the extracted NI current (curves I–III) and discharge voltage (U_d) on discharge current.
I – 3 slits 1x17mm², S_Σ =51mm²
II – 51 holes ø1,2mm, S_Σ =59mm²;
III – 48 holes ø0,8mm, S_Σ =25mm²;
I, II – Ta cathode, III – Moly cathode.

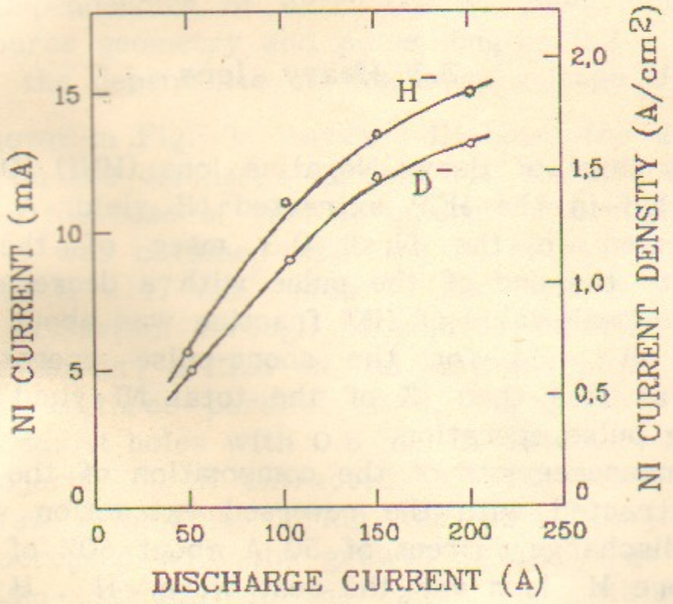

Fig.4. A plot of the extracted H^- and D^- ion current VS discharge current
1 emission hole ø1mm, β=60°, Δ=5,5mm.

3.4. Isotope effect

Fig. 4 shows the dependence of H^- and D^- ion current extracted from the source having one conical emission hole with permeable diameter of 1.0 mm. The HCP isotope effect was small - about 15% at discharge current of 200 A, and it was decreased with the decrease in discharge current. It was less than that in the previous measurements of isotope effect for a Penning SPS [7], but looks like the same measured for the honeycomb semiplanotron SPS [14]. Note, that a plasma density of a SPS deuterium discharge had the value approximately 1.4 times higher, than that for a hydrogen discharge (with the same discharge current). So, the measured low value of isotope effect shows, that HCP produced H^- (D^-) ions have either a high velocity during their moving through a dense plasma, or they have no motion through the dense plasma column.

3.5. Magnetic field and hydrogen pressure dependencies

The dependencies of HCP extracted H^- ion current on the magnetic field and discharge hydrogen pressure were different from those measured for the standard SPS.

In Fig. 5 are shown the dependencies of the NI yield I^-, discharge voltage U_d and positive ion current I^+, extracted with the reversed HCP extraction voltage vs an external magnetic field for a different spacing between an emission plate and the cathode edges. In the case of small spacing Z=1 mm (curves 1 in Fig. 5) an H^- yield and positive ion current onto an anode emission plate were increased and saturated with the growth of magnetic field. An initial growth of I^-, I^+, U_d values, recorded with a magnetic field increase was evidently caused by an increase in electron confinement in the discharge and by corresponding growth of the plasma density and an electrode particle bombardment intensity.

In the case of larger distance Z = 3 between the cathode edges and an emission plate (curves 2 in Fig. 5) the maximum value of I^- yield was achieved at the smaller and

optimal range of magnetic field 0.08 - 0.15 T. With further increase in magnetic field above the optimal value the H^- current was decreased. This decrease was presumably caused by the contraction of discharge and by a reduction of the plasma particle bombardment of the distant emission plate.

The positive ion current recorded with the reversed HCP extraction voltage had a value several times less then the extracted H^- current (Fig. 5 - 7,9). It clearly demonstrated that the positive ion bombardment of emission plate surface did not produce a noticeable contribution into production of extracted H^- current. Such a low value of positive ion current to an emission plate is also evidenced to a positive potential of the near-anode plasma with respect to an emission plate potential.

The dependencies of NI current I^-, positive ion current I^+, and discharge voltage U_d on the hydrogen pressure in the discharge region (measured during the discharge operation) are shown at Fig. 6. The indicated values of discharge hydrogen pressure was defined from the measurements of hydrogen flow made during the discharge operation. Discharge voltage and positive ion flux to emission plate were decreased with an increasing in the hydrogen density. The NI field was increased two times with the growth of hydrogen density. This dependence was in contrary to the same of the standard SPS.

The initial HCP hydrogen pressure, measured before the discharge switching on, as well as the pressure in the cathode hollows during the discharge operation, had a values several times higher than the hydrogen density in the discharge area during high-current operation.

This drop of hydrogen pressure between the cathode hollows and the discharge area recorded with the discharge switching on was caused by the locking the hydrogen in the cathode cavities by the plasma pressure, and was dependent of the discharge current and of the relative permeability of the cathode openings and the emission holes. Under the conditions of Fig. 6. the indicated value of hydrogen density in discharge was 3 - 5 times lower, than that before the discharge switching on.

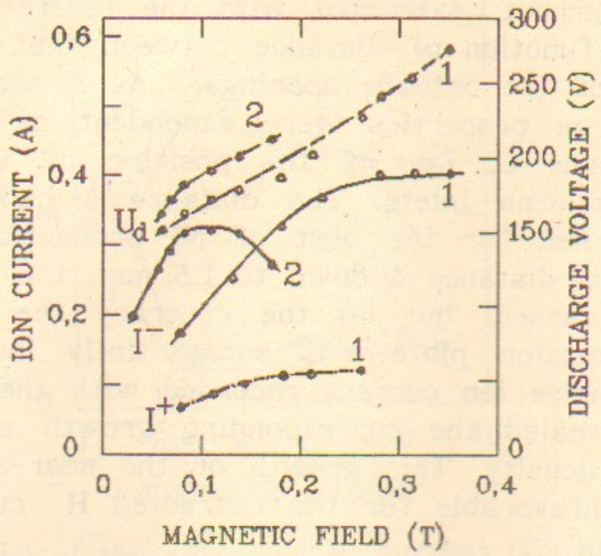

Fig.5. Dependencies of the extracted negative ion current I^-, positive ion current I^+ and discharge voltage U_d on magnetic field for different spacing Z between the cathode edge and the anode plate.
1 - Z=1mm, Δ=5,5mm; 2 - Z=3mm, Δ=1,5mm.

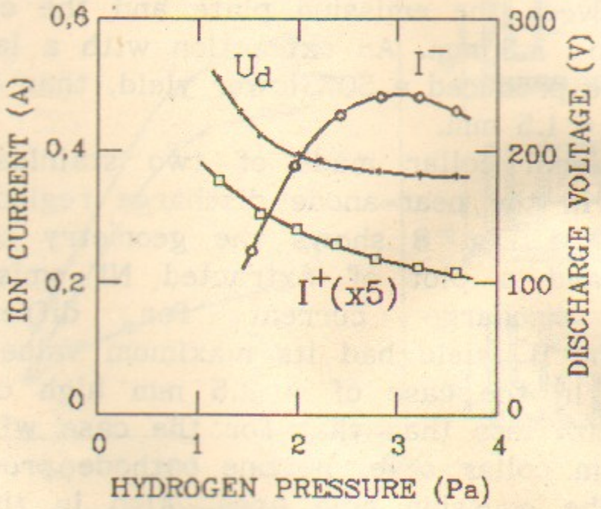

Fig.6. A plot of the extracted negative ion current (I^-), positive ion current (I^+) and discharge voltage (U_d) vs hydrogen pressure in the discharge region.

Fig. 7 shows a plot of the extracted NI current and of the positive current, extracted with the reversed extraction voltage, as a function of distance between the cathode edge and the axis of the cathode openings. As it seen from Fig. 7, the discharge properties were dependent of the cathode openings distance Δ, i.e. of the position of the hydrogen and primary plasma inlets. The distance Δ had an optimal value of 3-4 mm for the best of NI production. With the decrease in this distance Δ down to 1.5 mm, the extracted NI yield was decreased, but on the contrary the positive ion current to emission plate was substantially increased. The growth of positive ion current recorded with the decrease in distance Δ revealed the corresponding growth of the near-anode plasma density. This growth of the near-anode plasma density was unfavorable for the extracted H^- current intensity.

A different thickness of discharge column in the range 1.5 - 10 mm was tested at the different positions of anode insert with respect to cathode edges (δ in Fig. 2). The maximum H^- yield was obtained for an optimal value of $\delta \simeq 5$ - 7.5 mm. The H^- yield was 20% decreased with the growth of spacing Z between the emission plate and the cathode edges from 1.5 up to 3.5 mm. An extraction with a larger spacing Z = 8 mm have produced a 50% lower yield, than that obtained for spacing Z = 1.5 mm.

An additional collar made of two stainless steel fins was installed in the near-anode discharge region for the NI production study. Fig. 8 shows the geometry of the collar used (right) and a plot of extracted NI emission current density vs discharge current for different collar geometries. The H^- yield had its maximum value in the case of no collar. In the case of a 2.5 mm high collar the H^- yield was a 20% less than that for the case with no collar. In this 2.5 mm collar case, no one cathode produced H^- ion could reach the emission hole area. Also in this case, the flux of cathode produced fast hydrogen atoms illuminated the emission hole area with at least ten times less luminosity than that in the case with no collar.

Unexpectedly high NI yield with an emission current density of up to 0.6 A/cm^2 was extracted in the case of a

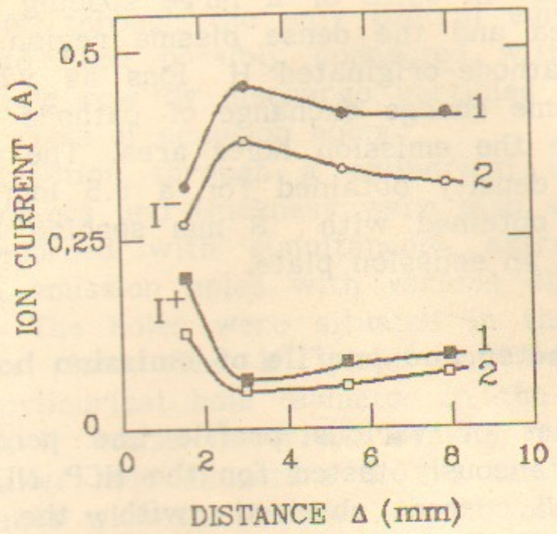

Fig.7. A graph of the extracted NI current (I^-) and of the positive ion current (I^+) as a function of distance Δ between the cathode openings and the cathode edge.
1 – discharge current 150A;
2 – discharge current 100A.

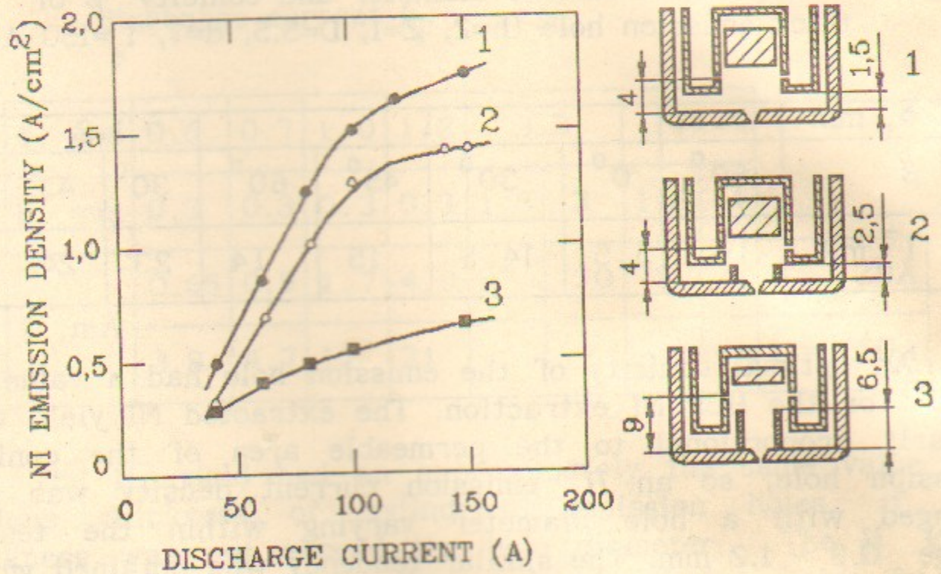

Fig.8. NI emission density as a function of the discharge current for various collar dimensions.

6.5 mm high collar in spite of a large spacing between the emission hole area and the dense plasma region.(Fig. 8). In this case, the cathode-originated H^- ions as well as those produced via volume charge exchange of cathode ions had no chance to achieve the emission holes area. The value of H^- emission current density obtained for a 6.5 mm collar was similar to those obtained with 8 mm spacing between the cathode edges and an emission plate.

3.7. Diameter and profile of emission holes

Emission holes of various profile and permeable diameter were simultaneously tested for the HCP NI extraction. A plot of the NI current obtained with the extraction through several thick (h=2 mm) emission holes of 0.8-1.2 mm in diameter and variable conicity of $\beta = 0 - 60^\circ$ is shown in Table 2. The emission holes were located in the central row of the emission plate.

Table 2. NI yield at various diameter and conicity β of thick emission hole (h=2, Z=1, D=5.5, d=7, I_d=150 A)

Φ, mm	0.8	1				1.2	
β	60^0	0^0	30^0	45^0	60^0	30^0	45^0
I^-,mA	10	5.5	14.5	15	14	23	24

An optimal conicity of the emission hole had a value of $\beta=45^\circ$ for the HCP NI extraction. The extracted NI yield was linearly proportional to the permeable area of the conical emission hole, so an H^- emission current density was not changed with a hole diameter varying within the tested range 0.8 - 1.2 mm. The similar tendency was obtained while using the full-scale multiaperture extraction through the conical emission holes (Fig. 3).

An average H^- yield, obtained during the multiaperture extraction and normalized to an emission hole number, had a

value approximately 1.5 times less than that obtained for the extraction through the only central emission holes. This reduction had been possibly connected with an illumination of central hole row by discharge particles higher, than that for the side rows of emission holes.

An extraction through a cylindrical emission holes of various diameters and thickness were also studied. A plot of NI yield recorded with simultaneous extraction through a several thin emission holes with various diameters is shown in Table 3. The holes were situated in the central row of the emission plate. The H^- yield was increased with the growth of cylindrical hole diameter in the tested range 0.6 - 7 mm. An H^- emission current density had the same value for the smaller hole diameters 0.6 -1 mm. It was increased 1.5 - 1.3 times with the further growth of hole diameter up to 1.2 and 3.5 mm. The maximum H^- emission current density was achieved at the emission hole diameter of 1.2 mm.

Table 3. NI yield I^- vs a diameter of cylindrical emission hole with different thickness h for two values of discharge current I_d.

Φ, mm	0.6	0.7	1.0	1.2	3.5		7		
h, mm	0.3	0.3	0.3	0.3	1.5	3	1.5	4	
I^-,mA	0.65	0.9	1.7	4.0	27	30	75	75	I_d= 20A
	3.8	4.7	12	21	-	-	-	-	I_d= 150A

The H^- yield had an approximately the same value for various thickness of cylindrical emission holes, if the thickness was not exceed the hole diameter. The H^- yield extracted through the thick conical emission holes had a value 25% higher, than that for a thin cylindrical hole with the same permeable diameter.

3.8. Emission plate temperature and biasing

A plot of the extracted NI current recorded for different temperatures of emission plate is shown in Fig.9. An emission plate temperature was changed in the range 260-500 °C by a compressed air cooling on/off. After the cooling off (left point indicated by an arrow) the emission plate temperature was gradually increased up to its constant level, defined by the used discharge power and a pulse repetition rate. During this emission plate temperature growth the H^- yield was 40% increased.

After the cooling on (right point) the emission plate temperature and H^- yield were decreased. The dependence in Fig.9 was similar to those, obtained by Y.Okumura et al [12] and was repeated in the several cycles of the heating and cooling. The hysteresis in Fig.9 was connected with the delayed change of temperature at the point of thermocouple

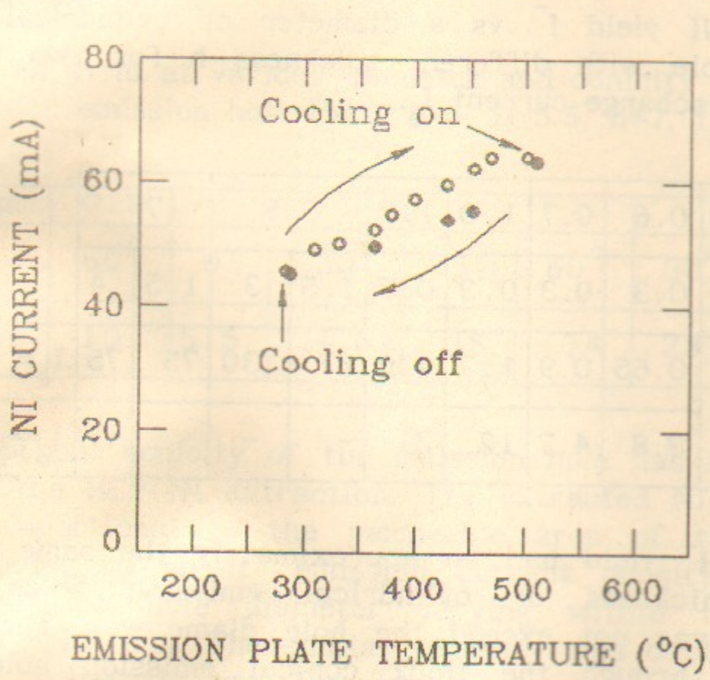

Fig.9. A plot of the extracted NI current vs anode emission plate temperature.
8 emission holes ⌀0,9mm, β=60°, Δ=5,5mm.

measurement (situated at the emission plate side) and the same at the operation area of the emission plate.

The discharge voltage, as well as the cathode and an anode insert temperatures were not changed while varying the emission plate temperature. So, the cesium volume density, a cesium coverage of the cathode and an anode insert and its corresponding H^- ion production were not changed during the rise of the emission plate temperature. It means that the pronounced 40% increase in H^- yield recorded with the temperature growth was connected with NI production on the emission plate surface. The H^- ion production was maximal at the higher emission plate temperature.

Fig. 10, 11 show the NI yield I^- and extraction circuit total current I_o as a function of emission plate bias with respect to an anode for the cases of the partial and multiaperture extraction. The negative bias of emission plate was more optimal for NI extraction, while the positive biasing led to NI yield decrease. For the larger value of emission plate negative bias of 80 V the recorded NI yield was decreased.

The floating bias of the emission plate had the value of 5 - 10 V negative with respect to an anode potential, so a negative (electron and NI) current was dominated in the charged particle flux onto the anode biased emission plate (for the distance Δ = 1.5-3 mm and magnetic field 0.1-0.3 T) An additional negative biasing 20-60 V of the emission plate with respect to an anode made the emission plate potential negative to vicinal plasma. It significantly increased the positive ion bombardment of emission plate and could improve a surface NI production.

3.9. Long-pulsed and DC-mode operation

The operation of small HCP source both in the long-pulsed and in DC-mode was studied. The hydrogen-cesium mode HC-1 with voltage of 90 V and current of up to 50 A was stably operated in the 1 sec pulse duration. The further increase in discharge current or in pulse duration was limited by an overheating of the noncooled cathodes and an anode insert. The full-scale multiaperture extraction produced the

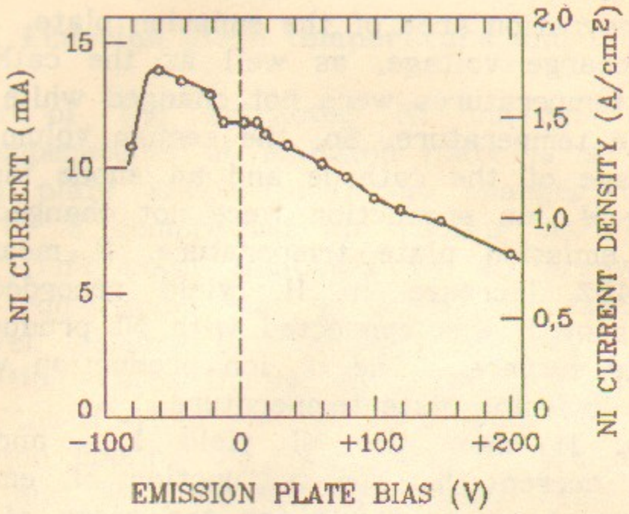

Fig.10. The extracted NI current and the corresponding NI current density in the emission hole vs emission plate bias with respect to anode.
Z=1mm, Δ=5,5mm; 1 emission hole ϕ1mm, β=60°

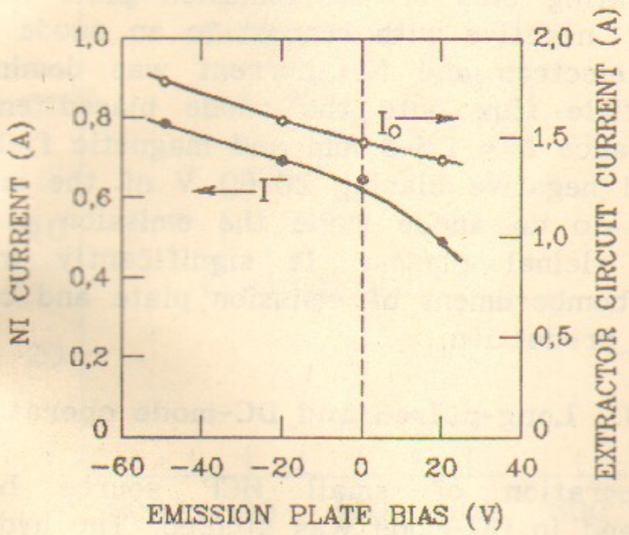

Fig.11. A plot of the extracted negative ion current (I^-) and of the extractor circuit current (I_o) as a function of the emission plate bias with respect to anode.
51 emission holes ϕ1,2mm, Δ=5,5mm.

H^- yield with intensity of 0.2 A (pulse duration 0.3 sec) while using 48 conical emission holes. This value was similar to those obtained with the short-pulse operation (see Fig.3). With the discharge current of 20 A and pulse duration of 60 sec an H^- yield with current of 0.1 A was obtained. In the last case the short-pulse extraction was used (1 msec pulse, repetition rate 100 Hz). Cesium coverage of HCP electrodes was stable and provided an intense invariable NI production. The summary of long-pulsed operation data are listed in Table 4.

Table 4. Data for the long-pulse operation

Discharge			Extraction			H^- current A
sec	current A	voltage V	sec	voltage kV	Hz	
1	50	90	0.3	17	0.1	0.2
60	20	70	10^{-3}	13	100	0.1

The stable DC operation of small HCP source was realized with a discharge power range of 0.1 - 0.3 kWt. Several discharge modes with various voltage and NI emission data were observed at different level of discharge power and Cs feeding. The data for various hydrogen-cesium discharge DC-modes are listed in Table 5. The H^- production rate increased with the growth of discharge voltage. In the standard HCP mode HC-I with a discharge voltage 60 - 160 V the H^- yield had a value higher, than that for an overcesiated

Table 5. H^- production I^- at various discharge voltage U_d and current I_d in the dc operation. 48 em. holes

I_d, A	6					5	2.5	2
U_d, V	15	20	30	40	50	60	120	160
I^-, mA	0.5	2	4	10	18	19	13	12

mode HC-II with a voltage 15 - 40 V. The noticeable H^- production was realized with a low discharge voltage of 15 V. The power efficiency of H^- production had its maximum value at discharge voltage of 60 V.

4. DISCUSSION

There are several processes can be responsible for an effective NI production in the HCP source:

a) A direct surface-plasma production due to particles reflection or impact desorption from the cathode, anode insert or emission plate surfaces;

b) A charge exchange of the surface produced NI in the volume of the plasma column or in the near-anode plasma.

4.1. The pure volume H^- production in hydrogen-cesium plasma due to collisions of hydrogen with cesium had no substantial contribution to the HCP H^- yield for the most efficient hydrogen-cesium mode HC-1. As it seen from Table 1, this surface-activated mode with a decreased cesium volume density had the H^- production rate much higher, than that for mode HC-II with larger cesium volume density. The recorded processes of SPS activation (modes H-II, HC-I) indicated directly to the surface production of the most of the initial H^- flux in HCP. This plasma-enhanced activation of the surface NI production is caused by the saturation of the surface selvage with hydrogen and by sputtering the excess of cesium and the impurities from the cesiated cathode and anode surfaces [15].

In principal the cathode-produced H^- ions, especially those produced due to reflection of fast positive ions or neutrals, could directly arrive to the HCP emission hole area with no collar. But the comparison of curves 1,2 in Fig. 8, as well as the data for thin and thick emission hole production (Tables 2,3) shows that the cathode-produced H^- ions have no essential income into HCP extracted H^- current. The only fast H^- ions, produced on the anode insert surface due to reflection of fast neutrals, could overcome the near-anode potential barrier and enter the plasma and extraction region.

4.2. The majority of the HCP extracted H^- ions was

produced due to a surface production of H^- ions on the emission hole cones or due to the resonant charge-exchange of these anode produced H^- ions in the vicinity of emission holes. It was confirmed by a 40% growth of H^- yield, recorded with the increase in an emission plate temperature, by the distinct increase in H^- yield recorded in the wide range of discharge current and plasma density (Fig. 3), by a decrease in H^- yield, recorded with an anode plasma density growth (Fig. 6,7), by a high value of H^- yield obtained in the cases of a 6.5 mm collar or 8 mm spacing between the cathode edges and an emission plate.

The superthermal and fast hydrogen atoms are responsible for an intense anode H^- production in HCP, since the positive ion bombardment of anode emission plate had a rather low value with respect to the H^- yield. An intense bombardment of the SPS anode surface by fast hydrogen atoms with a flux density of up to $1.6 \cdot 10^{19}$ cm^{-2} was measured [16] at discharge current density $\simeq$ 10 A/cm^2. An intense flux ($0.3 - 2 \cdot 10^{20}$ cm^{-2}) of hot hydrogen atoms (T_H = 1-2 eV) irradiates the SPS electrodes, as it reveals by spectroscopic measurements of Penning SPS atomic hydrogen density and temperature [17]. For the optimum cesium coverage on molybdenum the conversion of superthermal hydrogen atoms into the H^- ions has a rather high value of K^- = 0.04 H^- per incident atom with energy higher, than 1 eV [18].

The 15 - 20% growth of NI yield recorded with the negative bias of emission plate (Fig. 10,11) was naturally connected with an additional positive ion bombardment and an increased surface production of H^- ions. A negative biasing of 20 - 60 V of the emission plate with respect to an anode made the emission plate potential negative to vicinal plasma. It significantly increased the positive ion bombardment of emission plate and improved a surface NI production. For the negative bias of 80 V the recorded NI yield had a lower value (Fig. 10) possibly due to the sputtering of cesium coverage from an anode surface with the positive ions having an increased energy.

The H^- ion production was maximal at the higher emission plate temperature (Fig.9). It evidenced that the

condensation of cesium on emission plate surface during its cooling led to an overcesiation of the coverage above the value optimal for H^- production $\theta_{Cs} \simeq 0.6$ monolayer. Cesium coverage of hot HCP electrodes was stable and provided an intense invariable NI production in the long pulse and dc operation. The high stability of cesium coverage of the anode emission plate was caused by a low intensity and low energy of positive ion bombardment of the anode.

4.3. The most of H^- ions produced due to grazing atom reflection from the outer edges of emission hole cones could easy be extracted. (Fig. 12). A square growth of H^- yield recorded with the emission hole diameter increase shows, that a collecting of anode-produced H^- ions was improved with the growth of hole diameter. This increase of H^- ion collection was presumably caused by a volume charge exchange of H^- ions in the vicinity of extraction region due to the process:

$$H^- + H^0 \rightarrow H^0 + H^- \qquad (1)$$

A part of the anode-produced H^- flux was not directly extracted because of its moving out of the extraction region (Fig. 12). The volume charge exchange of anode-produced H^- ions can decrease their backflow out of the extraction region and correspondingly contribute to H^- yield with the partial return of the anode produced H^- flux into the formed H^- beam.

As it shown by Gealy and Van Zyl [19], the cross section of resonant charge exchange process (1) had an abnormally high value of $7 - 6 \cdot 10^{-15}$ cm^2 for H^- ion energy of 4 - 9 eV. Since the measured density of H^0 atom target in the extraction region of Penning SPS [17] had a high value of $4\text{-}5 \cdot 10^{14}$ cm^{-3}, the mean free path of anode-produced H^- ions before the charge exchange is only $\lambda = (n\sigma)^{-1} \simeq 4$ mm. It shows, that the partial return of H^- ions to emission aperture can be essential in the case of extraction through the holes with a large diameter. The H^- ions produced by a charge exchange still moving in the same direction, as the original hydrogen atoms, so the remarkable part of H^- ions produced by volume charge exchange in the vicinity of

emission hole moved to the extraction aperture and easy extracted.

The value of H^- yield, recorded for the slit extraction higher than that for extraction from the holes with the same permeable area was possibly connected with the better charge-exchange return of the anode-produced H^- ion flux into the long emission slit aperture. A collecting of H^- ions and an "efficient" emitting area of emission hole cones (L_{eff} in Fig.12) had a higher value for the optimal conicity of the emission holes. The growth of positive bias of emission plate with respect to anode and corresponding decrease of H^- yield (Fig. 10) was possibly connected by locking of anode-produced H^- ions near the surface and the worst partial return and collection of H^- ions to emission apertures in this case.

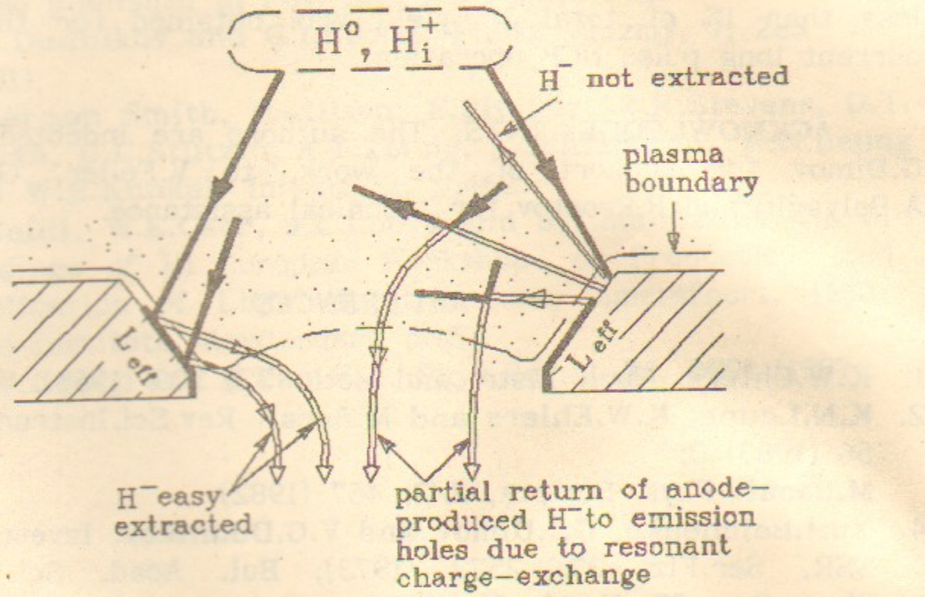

Fig.12. Mechanism of H^- ions production and collecting.
Filled lines – H^0 or H^+ trajectories.
Unfilled lines – H^- ions trajectories.
L_{eff} – an effective area with direct extraction of anode-produced H^- ions.

5. CONCLUSION

A small hollow cathode Penning SPS was developed and studied. The H^- yield was proportional to the emission aperture area and was increased in a wide range of discharge current. The H^- yield with an intensity of up to 0.95 A and an emission current density of up to 3.6 A/cm^2 was obtained in pulsed mode. Dependencies of H^- yield vs magnetic field and a hydrogen feed were differed from that of the standard Penning SPS. An optimal cesium coverage of the HCP electrodes was stable in the high-current long-pulsed operation as well as that in a dc source operation. An intense NI production was also obtained in long-pulse operation.

The most of extracted H^- ions were originated due to conversion of fast and superthermal atoms on the cesiated surfaces of emission hole cones. A low level of heavy NI less than 1% of total NI yield was obtained for the high-current long pulse HCP operation.

ACKNOWLEDGEMENTS. The authors are indebted to Pr. G.Dimov for support of the work, to V.Feller, G.Dolgov, A.Belyagin and P.Prostov for technical assistance.

REFERENCES

1. **K.W.Ehlers**. Nucl. Instr. and Meth. 32, 309 (1965).
2. **K.N.Leung, K.W.Ehlers and M.Bacal**. Rev.Sci.Instrum, 54, 56 (1983) 3;
   M.Bacal. Phys. Scripta, 2/2, 467 (1982).
4. **Yu.I.Belchenko, G.I.Dimov and V.G.Dudnikov**. Izvestiya AN SSR, Ser.Fiz. 37, 2573 (1973); Bul. Acad. Sci. USSR, Phys. Ser. 37, No.12, 91 (1973).
5. **Yu.I.Belchenko**. Investigations of Negative Ion Production in High-Current Discharges, Thesis, INP Novosibirsk, 1974 (in Russian).
6. **V.G.Dudnikov**. in Proceedings of the 4th All-Union Conference on Charged Particle Accelerators, Moscow, 1974 (Moscow, Nauka, 1975).
7. **K.Prelec**. Nucl. Instr. and Meth. 144, 413 (1977).

8. **G.I.Dimov, G.E.Derevyankin and V.G.Dudnikov**. IEEE Trans. Nucl. Sci. NS-24, 1545 (1977).
9. **P.Allison**. IEEE Trans.Nucl.Sci. NC-24, 1594 (1977).
10. **Yu.I.Belchenko, G.I.Dimov and V.G.Dudnikov**. Proceedings of the International Symposium on the Production and Neutralization of Negative Hydrogen Ions and Beams, BNL-50727 (New-York, 1977), p.79.
11. **S.R.Walther, K.N.Leung and W.B.Kunkel**, J. Appl. Phys. 64, 3424 (1988).
12. **Y.Okumura, M.Hanada, T.Inoue, H.Kojima, Y.Matsuda, Y.Ohara, M.Seki and K.Watanabe**. AIP Conference Proc.210, (New-York, 1990), p.169.
13. **Yu.I.Belchenko and A.S.Kupriyanov**. Rev. Phys. Appl. (Paris) 23, 1889, (1988).
14. **Yu.I.Belchenko**. Fizika Plazmy, 9, 1219 (1983).
15. **Yu.I.Belchenko**. Preprint INP 91-27, Novosibirsk, 1991, to be published in Rev. Sci. Instrum., 1992.
16. **V.G.Dudnikov and G.I.Fiksel**. Fizika Plazmy, 7, 283 (1981).
17. **H.Vernon Smith, P.Allison, E.Pitcher, R.R.Stevens, G.T. Worth, G.C.Stutzin, A.T.Young, A.Schlachter, K.N.Leung and W.B.Kunkel**. In: Ref.12, p.462.
18. **M.Seidl, W.E.Carr, J.L.Lopes and S.T.Melnichuk**. In: Proceedings of III European Workshop on Production and Application of Light Negative Ions, Amersfoort, 1988, FOM-Institute, Amsterdam, p.157.
19. **M.W.Gealy and B.Van Zyl**. Phys.Rev.A, 36, 3091 (1987).